

# Cross-validation based adaptive sampling for Gaussian process models

Hossein Mohammadi <sup>\*1, 2</sup>, Peter Challenor<sup>1, 2</sup>, Daniel Williamson<sup>1</sup>, and Marc Goodfellow<sup>1, 2</sup>

<sup>1</sup>College of Engineering, Mathematics and Physical Sciences, University of Exeter, Exeter, UK

<sup>2</sup>EPSRC Centre for Predictive Modelling in Healthcare, University of Exeter, Exeter, UK

## Abstract

In many real-world applications, we are interested in approximating black-box, costly functions as accurately as possible with the smallest number of function evaluations. A complex computer code is an example of such a function. In this work, a Gaussian process (GP) emulator is used to approximate the output of complex computer code. We consider the problem of extending an initial experiment (set of model runs) sequentially to improve the emulator. A sequential sampling approach based on leave-one-out (LOO) cross-validation is proposed that can be easily extended to a batch mode. This is a desirable property since it saves the user time when parallel computing is available. After fitting a GP to training data points, the expected squared LOO (ES-LOO) error is calculated at each design point. ES-LOO is used as a measure to identify important data points. More precisely, when this quantity is large at a point it means that the quality of prediction depends a great deal on that point and adding more samples nearby could improve the accuracy of the GP. As a result, it is reasonable to select the next sample where ES-LOO is maximised. However, ES-LOO is only known at the experimental design and needs to be estimated at unobserved points. To do this, a second GP is fitted to the ES-LOO errors and where the maximum of the modified expected improvement (EI) criterion occurs is chosen as the next sample. EI is a popular acquisition function in Bayesian optimisation and is used to trade-off between local/global search. However, it has a tendency towards exploitation, meaning that its maximum is close to the (current) “best” sample. To avoid clustering, a modified version of EI, called pseudo expected improvement, is employed which is more explorative than EI yet allows us to discover unexplored regions. Our results show that the proposed sampling method is promising.

---

<sup>\*</sup>Corresponding Author: h.mohammadi@exeter.ac.uk

**Keywords:** Adaptive sampling; Computer experiment; Leave-one-out cross-validation; Gaussian processes

## 1 Introduction

In many real-world applications, we are interested in predicting the output of complex computer models (or simulators) such as high fidelity numerical solvers. The reason is that such models are computationally intensive and we cannot use them to perform analysis that requires very many runs. One way to predict the model output is to use surrogate models also known as emulators which are constructed based on a limited number of simulation runs. Surrogates are fast to run and the analysis can be carried out on them, see e.g. [27, 46, 2]. Among different classes of surrogate models, Gaussian process (GP) emulators [38] have gained increasing attention due to their statistical properties such as computational tractability and flexibility. GPs provide a flexible paradigm to approximate any smooth, continuous function [33] thanks to the variety of covariance kernels available. Most importantly, the GP prediction is equipped with an estimation of uncertainty which reflects the accuracy of the prediction.

One factor that heavily affects the accuracy of emulators is the location of the training data, also called the design, [45, 21]. In this context, the design of computer experiments has become an integral part of the analysis of computer experiments [40, 41]. Generally speaking, such design can be performed in a *one-shot* or *adaptive* manner [28]. In the former all samples are chosen at once while in the latter the points are selected sequentially using information from the emulator and the existing data. Examples of one-shot design of experiments (DoEs) methods are the Latin hypercube [31], full factorial [6], orthogonal array [34], minimax and maximin-distance designs [17]. A potential drawback of one-shot DoEs is that they may result in under/oversampling and can waste computational resources [43, 11]. However, this is not the case for adaptive approaches where we can stop the computationally expensive sampling process as soon as the emulator reaches an acceptable level of accuracy. Moreover, with adaptive sampling it is possible to take more samples in “interesting” regions where, e.g., the underlying function is highly nonlinear or exhibits abrupt changes. This paper focuses on GP-based adaptive sampling where an initial design is extended sequentially to improve the emulator. The initial DoE is often *space-filling* meaning that the points are scattered uniformly over the input space. We refer the reader to [37, 20] and references therein for more information on space-filling designs.

There are various GP-based adaptive sampling methods which can be categorised according to their selection criteria, i.e. the strategies to find future designs. The readers are referred to [11, 28] for a comprehensive review of the existing methods. An intuitive criterion is the built-in predictive variance of GPs, also known as the prediction uncertainty or mean squared error (MSE). The idea is that the predictive variance is regarded as an estimation of the “real” prediction error and a point with the maximum uncertainty

is taken as the next experimental design [30, 16]. The predictive variance increases away from the data points. It is highly probable that sampling based on the MSE criterion gives some sort of space-filling design which can be achieved using one-shot techniques. Moreover, MSE is large on the boundaries of the input space and that can lead to taking a lot of samples on the boundaries. However, this is not desirable in many situations especially when the main characteristics of the true function appear inside the interior region and when the dimension of the input space is high. The integrated mean square error (IMSE) is a variant of the MSE criterion and selects a new point if adding that point to the existing design minimises the integral of the MSE [40, 35]. However, computing IMSE can be cumbersome, especially in high dimensions.

Maximum entropy is another common selection criterion in the adaptive sampling paradigm [44, 22]. It is equivalent to the maximum MSE criteria under certain circumstances [16, 24]. As a result, an adaptive sampling strategy based on maximum entropy tends to place many points at the borders of the input space [22]. This issue can be mitigated using *mutual information* (MI) as proposed by Krause et al. [23] in the sensor placement problem. The MI of two random variables is a measure of reduction in the uncertainty of one random variable through observing the other one. A sequential design approach is developed in [3] where the MI criterion is modified by introducing an extra parameter, called *nugget*, to the correlation matrix of the GP (in the denominator), see Appendix A. The inclusion of the nugget parameter prevents selecting a new sample close to the current design. The algorithm called MICE (mutual information for computer experiments) is then used to emulate a tsunami simulator.

The leave-one-out (LOO) cross-validation error defines another class of adaptive sampling criterion [26, 25, 1, 29]. To obtain the LOO error at an experimental design we remove that point from the training data set. Then, a GP is fitted to the remaining samples and the response at the left out point is predicted. The difference between the predicted and actual response serves as the LOO error. A relatively small error indicates that the prediction accuracy in a vicinity of the removed point is high and there is good information about the true function there. On the other hand, a comparably large error means that the removed point has a huge impact on the accuracy of the emulator and hence, we need more samples in the nearby region to reduce the errors. In [47] scores obtained by cross-validation are used to identify regions of distinct model behaviour and specify mixture of covariance functions for GP emulators. Using the LOO errors as a sampling criterion has several advantages. First, it provides actual prediction error at the design points. Second, it is model-independent and can be achieved by any surrogate model. For example, in [5] a methodology based on the LOO cross-validation is proposed to estimate the prediction uncertainty of any surrogate model, either deterministic or probabilistic. Third, computing the LOO errors is not expensive in terms of computational cost [8]. However, the LOO errors are not determined everywhere in the input space and only defined at locations where we have pre-existing model runs.

This paper proposes an adaptive sampling DoE relying on the LOO cross-validation

method to build GP emulators as accurately as possible for deterministic computer codes over the entire domain. The proposed method has a few parameters to be tuned and can be extended to a batch mode where at each iteration a set of inputs is selected for evaluation. This is an important property as it saves the user time when parallel computing is available [48]. The remainder of the paper is organised as follows. In the next section, the statistical methodology of GP emulators is briefly reviewed. Section 3 introduces the proposed adaptive sampling approach and its extension to batch mode. Section 4 presents numerical experiments where the predictive performance of our algorithm is tested. Finally, the paper's conclusion is in Section 5.

## 2 Gaussian process models

First we look at GP emulators and their statistical background. Let the underlying function of a deterministic complex computer code be given by  $f : \mathcal{D} \mapsto \mathbb{R}$  in which  $\mathcal{D}$  is a compact set in  $\mathbb{R}^d$ . Suppose  $\mathcal{A} = \{\mathbf{X}_n, \mathbf{y}_n\}$  is a training data set where  $\mathbf{X}_n = (\mathbf{x}_1, \dots, \mathbf{x}_n)^\top$  and  $\mathbf{y}_n = (f(\mathbf{x}_1), \dots, f(\mathbf{x}_n))^\top$  represent  $n$  locations in the input space  $\mathcal{D}$  and the corresponding outputs (responses/observations), respectively. Let  $(Z_0(\mathbf{x}))_{\mathbf{x} \in \mathcal{D}}$  be the Gaussian process by which we want to model  $f$ . In this framework, it is assumed that  $\mathbf{y}_n$  has a multivariate normal distribution given by

$$\mathbf{y}_n \sim \mathcal{N}(m_0(\mathbf{X}_n), k_0(\mathbf{X}_n, \mathbf{X}_n)), \quad (1)$$

where  $m_0$  and  $k_0$  are the (preselected) mean and covariance functions of  $(Z_0(\mathbf{x}))_{\mathbf{x} \in \mathcal{D}}$ . Without loss of generality, we assume that the mean function is a constant:  $m_0(x) = \mu$ . The positive semi-definite covariance function  $k_0$  plays an important role in GP modelling; assumptions about the underlying function such as differentiability or periodicity are encoded through kernels. The Matérn family of kernels are commonplace in computer experiments and (in the univariate case) are defined as

$$k_0(x, x') = \sigma^2 \frac{2^{1-\nu}}{\Gamma(\nu)} \left( \frac{\sqrt{2\nu}}{\theta} |x - x'| \right)^\nu B_\nu \left( \frac{\sqrt{2\nu}}{\theta} |x - x'| \right), \quad (2)$$

where  $\Gamma(\cdot)$  is the Gamma function and  $B_\nu(\cdot)$  denotes the modified Bessel function of the second kind of order  $\nu$ . The parameter  $\nu$  regulates the degree of smoothness of the GP sample paths/functions such that a process with the Matérn kernel of order  $\nu$  is  $\lfloor \nu - 1 \rfloor$  times differentiable [38]. The positive parameters  $\sigma^2$  and  $\theta$  are referred to as the *process variance* and *correlation length scale*, respectively. These parameters are usually unknown and need to be estimated from data. We refer the reader to [38, 12] for a more detailed explanation on parameter estimation techniques.

Given that the unknown parameters are estimated, the posterior predictive distribution relying on  $Z_n(\mathbf{x}) = Z_0(\mathbf{x}) \mid \mathcal{A}$  can be calculated. The posterior mean and covariance at a

generic location  $\mathbf{x}$  have closed-form expressions as [38]

$$m_n(\mathbf{x}) = \hat{\mu} + \mathbf{k}(\mathbf{x})^\top \mathbf{K}^{-1}(\mathbf{y}_n - \hat{\mu}\mathbf{1}) \quad (3)$$

$$k_n(\mathbf{x}, \mathbf{x}') = k_0(\mathbf{x}, \mathbf{x}') - \mathbf{k}(\mathbf{x})^\top \mathbf{K}^{-1} \mathbf{k}(\mathbf{x}') \\ + \frac{(1 - \mathbf{1}^\top \mathbf{K}^{-1} \mathbf{k}(\mathbf{x})) (1 - \mathbf{1}^\top \mathbf{K}^{-1} \mathbf{k}(\mathbf{x}'))}{\mathbf{1}^\top \mathbf{K}^{-1} \mathbf{1}}, \quad (4)$$

Here,  $\mathbf{k}(\mathbf{x}) = (k_0(\mathbf{x}, \mathbf{x}_1), \dots, k_0(\mathbf{x}, \mathbf{x}_n))^\top$  is the vector of covariances between  $Z_0(\mathbf{x})$  and  $Z_0(\mathbf{x}_i)$ s,  $\mathbf{1}$  is a vector of ones and  $\mathbf{K}$  is an  $n \times n$  covariance matrix with elements  $\mathbf{K}_{ij} = k_0(\mathbf{x}_i, \mathbf{x}_j)$ ,  $\forall 1 \leq i, j \leq n$ . The predictive variance  $s_n^2(\mathbf{x}) = k_n(\mathbf{x}, \mathbf{x})$  determines the uncertainty associated with the prediction at  $\mathbf{x} \in \mathcal{D}$  and is a measure of the prediction accuracy. In adaptive sampling based on the MSE criterion, the new sample is the point that maximises  $s_n^2(\mathbf{x})$ .

### 3 Proposed adaptive sampling method

Before introducing our method, it is worth mentioning that an “efficient” adaptive sampling strategy should meet the conditions below [28].

- (i) **Local exploitation:** that allows us to add more points in interesting areas discovered so far.
- (ii) **Global exploration:** by which unexplored domain regions can be detected.
- (iii) **Trade off between local exploitation and global exploration:** which balances the previous two objectives using a suitable measure.

The proposed adaptive sampling approach uses *expected squared LOO error*, see Section 3.1, for local exploitation. The global exploration and the trade off between the local/global search is driven by the *pseudo expected improvement* criterion introduced in Section 3.2.

#### 3.1 Expected squared LOO cross-validation error

We wish to improve the GP emulator  $Z_n(\mathbf{x})$  constructed on the training data set  $\mathcal{A}$  using the LOO cross-validation method. To do so, the first step is to obtain the LOO errors. Let  $e_L(\mathbf{x}_i)$  denote the LOO cross-validation error at the design sites  $\mathbf{x}_i, i = 1, \dots, n$ . The computation of  $e_L(\mathbf{x}_i)$  relies on the Gaussian process  $Z_{n,-i}(\mathbf{x})$  which is obtained by conditioning  $Z_0(\mathbf{x})$  on all observations except the  $i$ -th one:  $Z_{n,-i}(\mathbf{x}) = Z_0(\mathbf{x}) \mid \mathbf{y}_n \setminus \{f(\mathbf{x}_i)\}$ . The predictive mean and variance of  $Z_{n,-i}(\mathbf{x})$  are shown by  $m_{n,-i}(\mathbf{x})$  and  $s_{n,-i}^2(\mathbf{x})$ , respectively. The LOO cross-validation error is then calculated as

$$e_L(\mathbf{x}_i) = |m_{n,-i}(\mathbf{x}_i) - f(\mathbf{x}_i)|, \quad (5)$$

which can be regarded as the sensitivity of the emulator to the left out point  $\mathbf{x}_i$ . As a result, the idea of adding new samples near the points with large LOO errors is used in several adaptive sampling works, see e.g. [26, 1]. In this work, we use the estimated parameters of  $Z_n(\mathbf{x})$  to fit  $Z_{n,-i}(\mathbf{x})$  and do not re-estimate them in order to alleviate the computational burden. Moreover, Equation (5) can be calculated efficiently using the formula proposed in [8].

The LOO error  $e_L(\mathbf{x}_i)$  only accounts for the difference between the predictive mean and the real value at  $\mathbf{x}_i$  and can be a misleading selection criterion in some situations. Figure 1 shows an example where the prediction at  $x_5 = 0$  is equal to the true value there and therefore  $e_L(x_5) = 0$ . This means that the chance of adding a new sample near the fifth data point is low although it is in a crucial region. The above mentioned problem can be mitigated using “expected squared LOO error (ES-LOO)” which provides more information than the LOO error about the sensitivity of the emulator to the design points. More precisely, ES-LOO accounts for both the prediction uncertainty and the difference between the prediction and the true value, as described below.

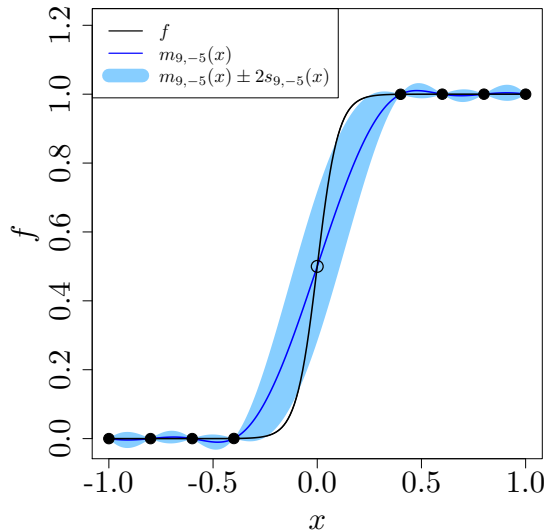


Figure 1: The LOO error (Equation (5)) can be misleading as a selection criterion. Removing the fifth sample, i.e.  $(0, 0.5)$ , does not change the prediction at  $x = 0$  and the LOO error remains zero there:  $|m_{9,-5}(x_5) - f(x_5)| = 0$ . This means that the point  $(0, 0.5)$  does not have any influence on the emulator while  $f$  has a large gradient there. However, the expected squared LOO error which accounts for the prediction uncertainty is not zero at  $x_5$ . The true function is  $f(x) = \frac{1}{1+\exp(-20x)}$ .

Let  $\mathcal{E}_L(\mathbf{x}_i)$  represent the value of ES-LOO error at the design site  $\mathbf{x}_i$ . It is defined as

$$\mathcal{E}_L(\mathbf{x}_i) = \frac{\mathbb{E} \left[ (Z_{n,-i}(\mathbf{x}_i) - f(\mathbf{x}_i))^2 \right]}{\sqrt{\text{Var} \left( (Z_{n,-i}(\mathbf{x}_i) - f(\mathbf{x}_i))^2 \right)}}, \quad (6)$$

where

$$\mathbb{E} \left[ (Z_{n,-i}(\mathbf{x}_i) - f(\mathbf{x}_i))^2 \right] = s_{n,-i}^2(\mathbf{x}_i) + (m_{n,-i}(\mathbf{x}_i) - f(\mathbf{x}_i))^2, \quad (7)$$

$$\text{Var} \left( (Z_{n,-i}(\mathbf{x}_i) - f(\mathbf{x}_i))^2 \right) = 2s_{n,-i}^4(\mathbf{x}_i) + 4s_{n,-i}^2(\mathbf{x}_i)(m_{n,-i}(\mathbf{x}_i) - f(\mathbf{x}_i))^2. \quad (8)$$

To see how the above equations are obtained we first note that

$$Z_{n,-i}(\mathbf{x}_i) \sim \mathcal{N} (m_{n,-i}(\mathbf{x}_i), s_{n,-i}^2(\mathbf{x}_i)), \quad (9)$$

as is shown with an example in Figure 2. By standardizing the above equation we reach

$$\frac{Z_{n,-i}(\mathbf{x}_i) - f(\mathbf{x}_i)}{s_{n,-i}(\mathbf{x}_i)} \sim \mathcal{N} \left( \frac{m_{n,-i}(\mathbf{x}_i) - f(\mathbf{x}_i)}{s_{n,-i}(\mathbf{x}_i)}, 1 \right), \quad (10)$$

in which the square of the left hand side is a random variable with noncentral chi-square distribution characterised by

$$\left( \frac{Z_{n,-i}(\mathbf{x}_i) - f(\mathbf{x}_i)}{s_{n,-i}(\mathbf{x}_i)} \right)^2 \sim \chi'^2 \left( \kappa = 1, \lambda = \left( \frac{m_{n,-i}(\mathbf{x}_i) - f(\mathbf{x}_i)}{s_{n,-i}(\mathbf{x}_i)} \right)^2 \right). \quad (11)$$

Here,  $\kappa$  and  $\lambda$  are the degrees of freedom and noncentrality parameter, respectively<sup>1</sup>. As a result

$$\mathbb{E} \left[ \left( \frac{Z_{n,-i}(\mathbf{x}_i) - f(\mathbf{x}_i)}{s_{n,-i}(\mathbf{x}_i)} \right)^2 \right] = 1 + \left( \frac{m_{n,-i}(\mathbf{x}_i) - f(\mathbf{x}_i)}{s_{n,-i}(\mathbf{x}_i)} \right)^2, \quad (12)$$

$$\text{Var} \left( \left( \frac{Z_{n,-i}(\mathbf{x}_i) - f(\mathbf{x}_i)}{s_{n,-i}(\mathbf{x}_i)} \right)^2 \right) = 2 \left( 1 + 2 \left( \frac{m_{n,-i}(\mathbf{x}_i) - f(\mathbf{x}_i)}{s_{n,-i}(\mathbf{x}_i)} \right)^2 \right). \quad (13)$$

Finally, if the expectation and variance in the above equations are multiplied by  $s_{n,-i}^2(\mathbf{x}_i)$ , we reach Equations (7) and (8).

The analytical expression of Equation (7) is similar to the *expected improvement for global fit (EIGF)* infill sampling criterion proposed by Lam [24]. In Section 4, we compare

---

<sup>1</sup>Suppose  $X_1, \dots, X_\kappa$  are  $\kappa$  independent random normal variables such that  $X_i \sim \mathcal{N}(\mu_i, 1), 1 \leq i \leq \kappa$ . Then,  $\sum_{i=1}^{\kappa} X_i^2 \sim \chi'^2(\kappa, \lambda = \sum_{i=1}^{\kappa} \mu_i^2)$  has a noncentral chi-square distribution with mean  $\kappa + \lambda$  and variance  $2(\kappa + 2\lambda)$ .

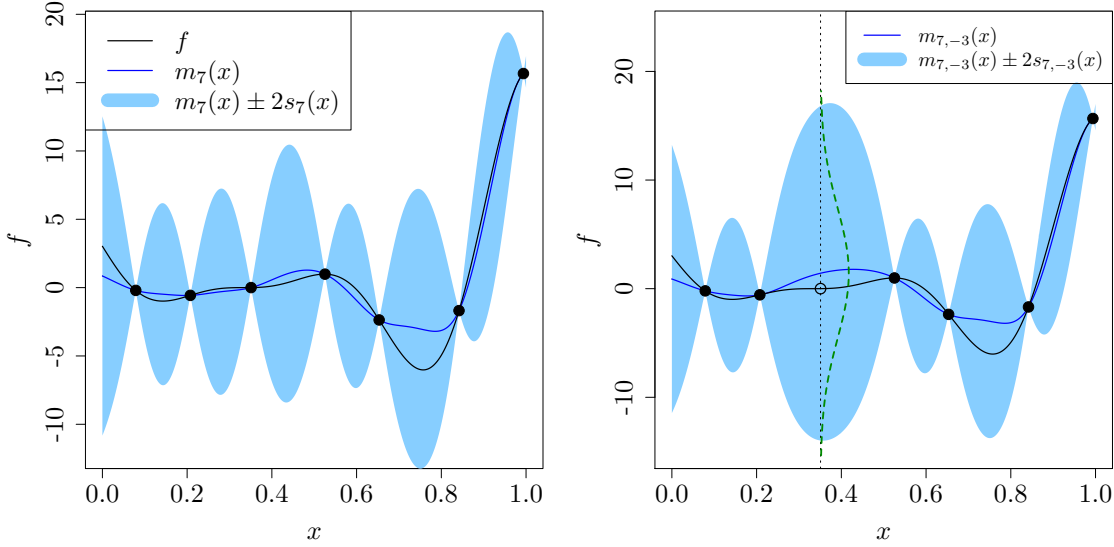


Figure 2: Left: Gaussian process prediction (blue) with 95% credible intervals (shaded) based on 7 observations from the true function (black). Right: GP prediction based on the training data except the third one where the GP has a normal distribution specified by Equation (9).

the predictive performance of our method with EIGF on several test functions. In EIGF, the improvement at an arbitrary point  $\mathbf{x}$  is given by:

$$IGF(\mathbf{x}) = (Z_n(\mathbf{x}) - f(\mathbf{x}_i^*))^2, \quad (14)$$

where  $f(\mathbf{x}_i^*)$  is the response at the location  $\mathbf{x}_i^*$  which is closest (in Euclidean distance) to  $\mathbf{x}$ . The EIGF criterion is the expected value of  $IGF(\mathbf{x})$  and takes the following form

$$EIGF(\mathbf{x}) = \mathbb{E}[IGF(\mathbf{x})] = (m_n(\mathbf{x}) - f(\mathbf{x}_i^*))^2 + s_n^2(\mathbf{x}). \quad (15)$$

Using EIGF as the selection criterion, the next sample is chosen where EIGF is maximum:

$$\mathbf{x}_{n+1} = \underset{\mathbf{x} \in \mathcal{D}}{\operatorname{argmax}} EIGF(\mathbf{x}).$$

### 3.2 Proposed selection criterion

Since the magnitude of  $\mathcal{E}_L(\mathbf{x}_i)$  reflects the sensitivity of the emulator to the loss of information provided by the function evaluation at  $\mathbf{x}_i$ , it is reasonable to choose the next sample where ES-LOO is maximum. However, this quantity is only defined at the training data while we need to look for the next design point out-of-sample. In this work, we extend the

ES-LOO error to be a function defined over the whole domain,  $\mathcal{E}_L(\mathbf{x}), \mathbf{x} \in \mathcal{D}$ , that we have observed at the design points, and we model this function with a GP. The interpretation of  $\mathcal{E}_L(\mathbf{x})$  is the value of the ES-LOO error we think we would see if  $(\mathbf{x}, f(\mathbf{x}))$  were part of our data set. The GP model to estimate  $\mathcal{E}_L(\mathbf{x})$  at unobserved locations is denoted by  $Z_n^e(\mathbf{x})$  whose predictive mean and variance are indicated by  $m_n^e(\mathbf{x})$  and  $s_n^e(\mathbf{x})$ , respectively. The training set for the second GP is  $\{\mathbf{X}_n, \mathbf{y}_n^e\}$  where  $\mathbf{y}_n^e = (\mathcal{E}_L(\mathbf{x}_1), \dots, \mathcal{E}_L(\mathbf{x}_n))^\top$ .

After estimating  $\mathcal{E}_L(\mathbf{x})$ , we can find its maximum applying techniques in surrogate-based optimisation. In this framework, a naive approach is to maximise  $m_n^e(\mathbf{x})$ . However, this simple strategy does not define a valid optimisation scheme due to *overexploitation* [18] meaning that the new samples are taken very close to the points with a large ES-LOO error. To overcome this problem, we need to take into account  $s_n^e(\mathbf{x})$  as the exploration component in the course of the search. To this end, we employ *Expected improvement (EI)* which is one of the most common acquisition functions in Bayesian optimisation [7, 18] to trade-off between exploration and exploitation. It is expressed via

$$EI(\mathbf{x}) = \begin{cases} (m_n^e(\mathbf{x}) - \max(\mathbf{y}_n^e)) \Phi(u) + s_n^e(\mathbf{x}) \phi(u) & \text{if } s_n^e(\mathbf{x}) > 0 \\ 0 & \text{if } s_n^e(\mathbf{x}) = 0, \end{cases} \quad (16)$$

where  $u = \frac{m_n^e(\mathbf{x}) - \max(\mathbf{y}_n^e)}{s_n^e(\mathbf{x})}$  and  $\phi(\cdot)$  and  $\Phi(\cdot)$  represent the PDF and CDF of the standard normal distribution, respectively. EI is a non-negative, parameter-free function and is zero at the data points. However, it is shown that EI is biased towards exploitation especially at the beginning of the search [42, 19, 36]. As a result, if EI is used to find the maximum of  $\mathcal{E}_L(\mathbf{x})$  at each iteration, the new samples are clustered. This is illustrated by an example in Figure 3 where the black circles are the initial design and the red circles represent the new samples selected based on the EI criterion. Clusters of the new points can be detected on the contour plot of Franke's function (its analytic expression is given in Appendix B) due to the tendency of EI towards exploitation.

In this paper, *pseudo expected improvement (PEI)* [49] is considered as the selection criterion which has a better exploration property than EI. Pseudo expected improvement is obtained by multiplying EI by a repulsion function (RF):  $PEI(\mathbf{x}) = EI(\mathbf{x})RF(\mathbf{x})$ . The repulsion function is defined as

$$RF(\mathbf{x}; \mathbf{X}_n) = \prod_{i=1}^n [1 - \text{Corr}(Z_n^e(\mathbf{x}), Z_n^e(\mathbf{x}_i))], \quad (17)$$

where  $\text{Corr}(\cdot, \cdot)$  is the correlation function of  $Z_n^e(\cdot)$ .  $RF(\mathbf{x})$  is a measure of the (canonical) distance between  $\mathbf{x}$  and the design points. It is always between zero and one and zero at the data points because  $\text{Corr}(Z_n^e(\mathbf{x}_i), Z_n^e(\mathbf{x}_i)) = 1, \forall \mathbf{x}_i \in \mathbf{X}_n$ . Multiplying EI by the repulsion function improves its exploration property as is shown in Figure 4. The picture on the left illustrates a GP fitted on five data points and the corresponding repulsion function (red), EI (blue) and PEI (black) are visualised on the right picture. It can be seen that the maximum of EI is biased towards the design point whose ES-LOO error is maximum.

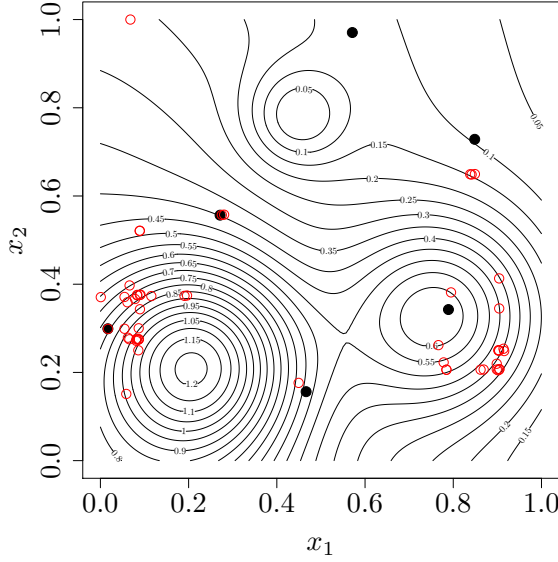


Figure 3: Adaptive designs (red circles) are obtained by maximising  $\mathcal{E}_L(\mathbf{x})$  using the EI criterion. The filled circles are the initial design and the true function is Franke's function. EI tends towards exploitation and as a result clustering occurs.

The correlation function in Equation (17) depends on length-scales  $\boldsymbol{\theta}^e = [\theta_1^e, \dots, \theta_d^e]^\top$  that are estimated from  $\{\mathbf{X}_n, \mathbf{y}_n^e\}$ . It is important that  $\theta_i^e$ 's do not take very “small” values to circumvent clustering. The reason is that when they come near zero,  $\text{Corr}(Z_n^e(\mathbf{x}), Z_n^e(\mathbf{x}_i))$  tends to zero and  $RF(\mathbf{x})$  is (almost) one everywhere meaning that it has no influence on EI. Besides, the maximum of EI is located in a shrinking neighbourhood of the current best point when  $\boldsymbol{\theta}^e$  is small [32]. Therefore, a lower bound has to be considered for  $\boldsymbol{\theta}^e$ . In a normalised input space, i.e.  $\mathcal{D} = [0, 1]^d$ , we define this lower bound to be

$$\theta_{lb}^e = \sqrt{-0.5 / \ln(10^{-8})}, \quad (18)$$

for each dimension. It is obtained by setting the minimum correlation equal to  $10^{-8}$  for the squared exponential correlation function defined as

$$k_0(x, x') = \exp\left(-\frac{|x - x'|^2}{2\theta^2}\right). \quad (19)$$

In the above equation, the minimum correlation between  $x$  and  $x'$  happens when  $|x - x'| = 1$  which is the maximum distance between the two points in the normalised input space.

A common issue in adaptive sampling strategies is that many design points lie along the boundaries of the input space where the predictive variance is large. Such samples might be nonoptimal if the true model is not feasible on the boundaries [13]. However,

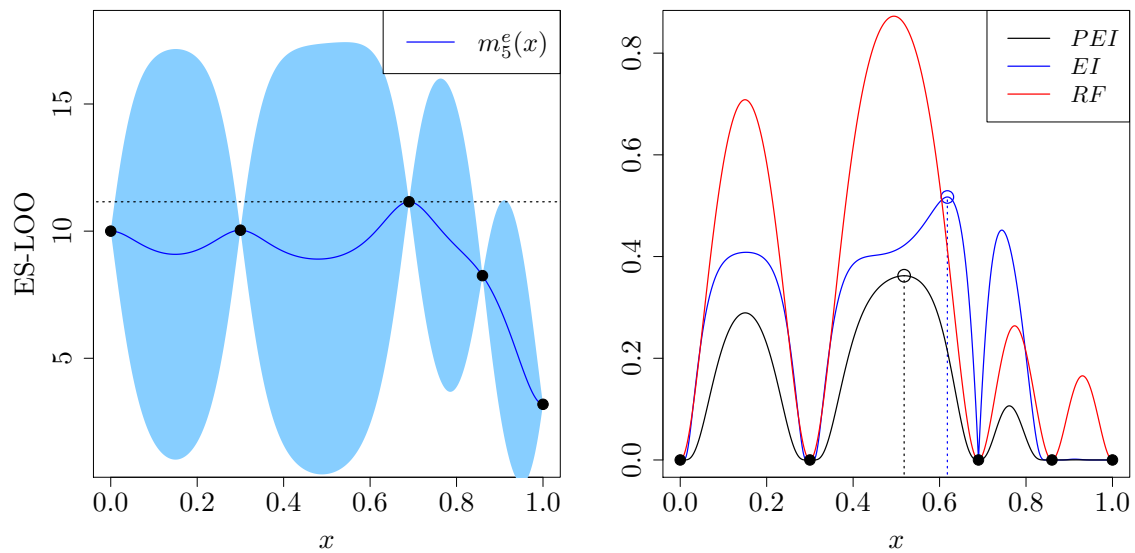


Figure 4: Left: A GP is fitted to five expected squared LOO errors. Right: Pseudo expected improvement (black) is obtained by multiplying expected improvement (blue) by the influence functions (red). The next sample point is where the PEI is maximum (black circle). The maximum of EI is shown by the blue circle. The PEI criterion is more explorative than EI.

this problem can be alleviated in our approach by introducing ‘‘pseudo points’’ at appropriate locations on the boundaries. Pseudo points, denoted by  $\mathbf{X}_p$ , are used to update the repulsion function, i.e.  $RF(\mathbf{x}; \mathbf{X}_n \cup \mathbf{X}_p)$ , but the true function is not evaluated there due to computational cost. The following locations are considered as the pseudo points in our algorithm

1. corners of the input space,
2. closest point on each face of the (rectangular) bounding input region to the initial design.

A 2-dimensional example is illustrated in Figure 5 that shows the location of pseudo points (red triangles) and six initial design (black points). Finally, Algorithm 1 summarises the steps of the proposed adaptive sampling method.

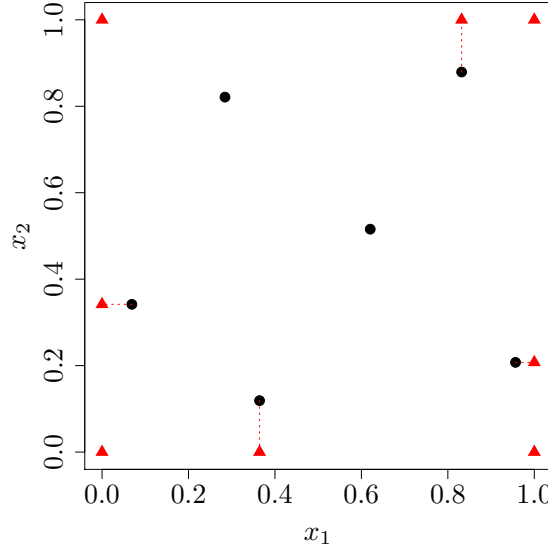


Figure 5: Initial design (black points) and pseudo points (red triangles). They are closest point on each face of the input space to the initial design and also at the corners of the region. The repulsion function is updated by pseudo points at almost no cost.

### 3.3 Extension to batch mode

When parallel computing is available, it is often better to evaluate the expensive function  $f$  at a set of inputs rather than a single point since it saves the user time. In batch sampling,  $q > 1$  locations are chosen for evaluation at each iteration. Note that the computation time of running the simulator on  $q$  parallel cores is the same as a single run. The PEI criterion

---

**Algorithm 1** Proposed sequential sampling approach

---

```

1: Create an initial design:  $\mathbf{X}_n = \{\mathbf{x}_1, \dots, \mathbf{x}_n\}$ 
2: Evaluate  $f$  at  $\mathbf{X}_n$ :  $\mathbf{y}_n = f(\mathbf{X}_n)$ 
3: Fit the GP  $Z_n(\mathbf{x})$  to  $\{\mathbf{X}_n, \mathbf{y}_n\}$ 
4: while not stop do
5:   for  $i = 1$  to  $n$  do
6:     Calculate  $\mathcal{E}_L(\mathbf{x}_i)$  (Equation (6))
7:   end for
8:   Set  $\mathbf{y}_n^e = (\mathcal{E}_L(\mathbf{x}_1), \dots, \mathcal{E}_L(\mathbf{x}_n))^\top$ 
9:   Set the lower bound for  $\theta^e$  (Equation (18))
10:  Fit the GP  $Z_n^e(\mathbf{x})$  to  $\{\mathbf{X}_n, \mathbf{y}_n^e\}$ 
11:  Create pseudo points  $\mathbf{X}_p$  (see Figure 5)
12:   $\mathbf{x}_{n+1} \leftarrow \underset{\mathbf{x} \in \mathcal{D}}{\operatorname{argmax}} PEI(\mathbf{x}) = EI(\mathbf{x})RF(\mathbf{x}; \mathbf{X}_n \cup \mathbf{X}_p)$ 
13:  Set  $\mathbf{X}_n = \mathbf{X}_n \cup \{\mathbf{x}_{n+1}\}$ 
14:  Evaluate  $f$  at  $\mathbf{x}_{n+1}$  and  $y_{n+1} \leftarrow f(\mathbf{x}_{n+1})$ 
15:  Set  $\mathbf{y}_n = \mathbf{y}_n \cup \{y_{n+1}\}$ 
16:  Update  $Z_n(\mathbf{x})$  using  $(\mathbf{x}_{n+1}, y_{n+1})$ 
17:   $n \leftarrow n + 1$ 
18: end while

```

---

can be employed in a batch mode thanks to the repulsion function. We now show how to choose  $q$  points  $\mathbf{x}_{n+1}, \dots, \mathbf{x}_{n+q}$  in a single iteration. The first point  $\mathbf{x}_{n+1}$  is obtained by maximising the PEI criterion. Then, the repulsion function is updated by  $\mathbf{x}_{n+1}$

$$RF(\mathbf{x}; \mathbf{X}_n \cup \mathbf{x}_{n+1}) = \prod_{i=1}^{n+1} [1 - \operatorname{Corr}(Z_n^e(\mathbf{x}), Z_n^e(\mathbf{x}_i))], \quad (20)$$

which updates PEI without evaluating  $f$  at  $\mathbf{x}_{n+1}$ . The second location  $\mathbf{x}_{n+2}$  is selected where the updated PEI is maximum. We repeat this procedure until the last point  $\mathbf{x}_{n+q}$  is chosen

$$RF(\mathbf{x}; \mathbf{X}_n \cup \mathbf{x}_{n+1} \cup \dots \cup \mathbf{x}_{n+q-1}) = \prod_{i=1}^{n+q-1} [1 - \operatorname{Corr}(Z_n^e(\mathbf{x}), Z_n^e(\mathbf{x}_i))]$$

$$\mathbf{x}_{n+q} = \underset{\mathbf{x} \in \mathcal{D}}{\operatorname{argmax}} EI(\mathbf{x})RF(\mathbf{x}; \mathbf{X}_n \cup \mathbf{x}_{n+1} \cup \dots \cup \mathbf{x}_{n+q-1}).$$

Figure 6 shows our adaptive sampling method in batch mode where  $q = 3$  locations ( $x_6, x_7$  and  $x_8$ ) are picked in one iteration. The first new sample  $x_6$  is chosen where the PEI criterion is maximum (left). Then, the repulsion function is updated by  $x_6$ . This will update PEI and its maximum allows us to find  $x_7$  without evaluating  $f$  at  $x_6$  (middle).

Again, we update the repulsion function using  $x_7$  and maximise the updated PEI to obtain the sample site  $x_8$  (right).

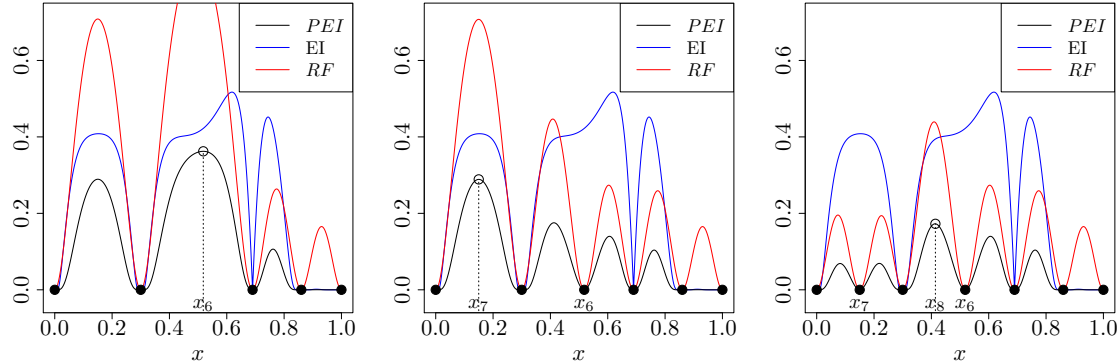


Figure 6: A batch of  $q = 3$  points ( $x_6, x_7$  and  $x_8$ ) are selected thanks to the repulsion function. Left: there are five initial samples and the first query point,  $x_6$ , is chosen where PEI is maximum. Middle: the repulsion function is updated as  $RF(x; x_{1:5} \cup x_6)$  which updates PEI accordingly without evaluating  $f$  at  $x_6$ . The second query point,  $x_7$ , is the location of maximum of updated PEI. Right: PEI is updated using  $x_7$  and the third sample,  $x_8$ , is selected as explained.

## 4 Numerical experiments

Experimental results are presented and discussed in this section. Four analytic test functions and two real-world problems are considered as the “true” function to asses the efficiency of our proposed sampling method. The results are compared with one-shot Latin hypercube sampling (LHS) and three adaptive approaches, namely MSE, EIGF and MICE. A typical characteristic of these adaptive sampling approaches is exhibited in Figure 7 where the black dots are the initial design (identical in all pictures) and the red circles represent the adaptive samples. The true function has two spikes as it is a sum of two Gaussian functions centred at  $(1/3, 1/3)^\top$  and  $(2/3, 2/3)^\top$ . As can be seen, our proposed method fills space uniformly with a focus on areas where the true function has nonlinear behaviour. EIGF tends toward local exploitation and does not explore the input space; it gets stuck in an optimum. MSE samples most points on the boundaries where the prediction uncertainty is large. It is possible that MSE leads to a space-filling design as is the case of the Franke’s function, see below. No special trend can be found on the performance of the MICE algorithm. However, it avoids sampling around the boundaries and all new points are taken in the interior region. We describe our implementation of ES-LOO below.

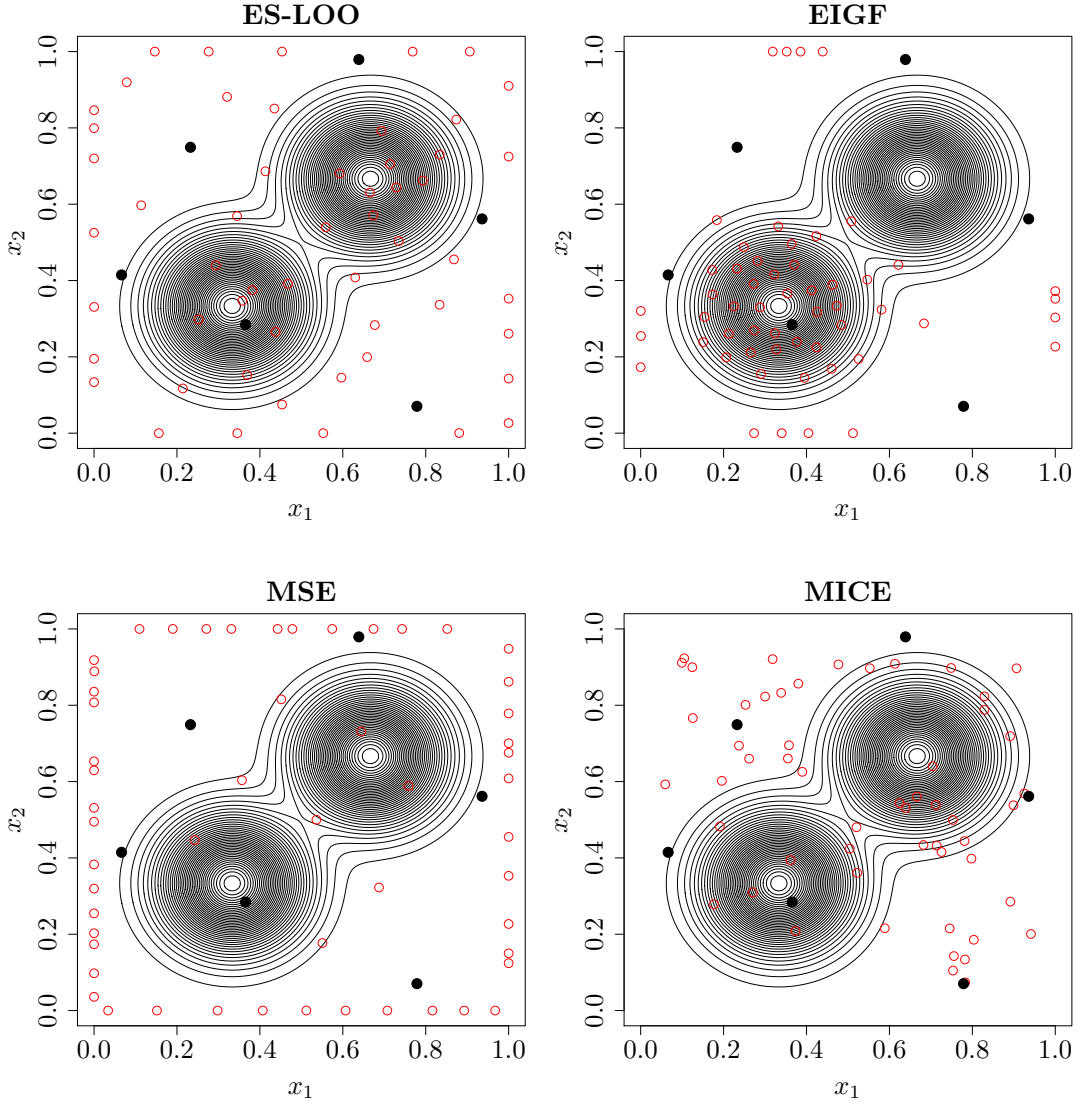


Figure 7: A typical sampling behaviour of four adaptive sampling methods: ES-LOO, EIGF, MSE and MICE. The red circles represent adaptive samples that are added to the six initial design (black dots). ES-LOO tends to fill the space with focusing on regions where the function values change rapidly. EIGF mainly exploits the basin of attraction of an optima while other areas are unexplored. MSE samples more points on the boundaries where the prediction uncertainty is large. There is not any special pattern in the sampling behaviour of MICE, however, it avoids to put points on the boundaries.

## 4.1 Experimental setup

The prediction accuracy is assessed by the *root mean squared error (RMSE)* criterion. Given the test set  $\{(\mathbf{x}_t, f(\mathbf{x}_t))\}_{t=1}^{t=N}$ , RMSE is defined as

$$RMSE = \sqrt{\frac{\sum_{t=1}^N (m_n(\mathbf{x}_t) - f(\mathbf{x}_t))^2}{N}}, \quad (21)$$

which measures the distance between the emulator,  $m_n(\mathbf{x}_t)$ , and the true function,  $f(\mathbf{x}_t)$ . In our experiments,  $N = 3000$  and the test points are selected uniformly across the input space. A total budget equal to  $30d$  is considered for each experiment. The initial space-filling DoE is of size  $3d$  and is obtained by the `maximinESE.LHS` function implemented in the R package *DiceDesign* [9]. There are ten different initial DoEs for every function and we asses the prediction performance of each method using all ten sets. The R package *DiceKriging* [39] is employed to construct GP models. The covariance kernel for modelling the true function and  $\mathcal{E}_L(\mathbf{x})$  is Matérn with  $\nu = 3/2$ . Since the ES-LOO error is a positive quantity, the GP emulator is fitted to its natural logarithm. The closest point on each face of the input space to the initial design and the corners of the input region are considered as the pseudo points.

## 4.2 Test functions

The four test functions are

- $f_1(\mathbf{x})$ : Franke's function [14],  $d = 2$
- $f_2(\mathbf{x})$ : Hartman function [15],  $d = 3$
- $f_3(\mathbf{x})$ : Friedman function [10],  $d = 5$
- $f_4(\mathbf{x})$ : Gramacy & Lee function [13],  $d = 6$

and their analytic expression are given in Appendix B. The four test functions are defined on  $[0, 1]^d$ . Figure 8 illustrates the prediction performance of our proposed method ES-LOO: sequential (black) and batch with  $q = 4$  (orange), MSE (blue), EIGF (red) and MICE (green). Each curve represents the median of ten RMSEs using ten different initial DoEs. The  $x$ -axis shows the number of function evaluations divided by the problem dimension,  $d$ . The  $y$ -axis is on logarithmic scale. The dashed grey lines are the median of RMSEs based on one-shot LHS of sizes (from top to bottom):  $10d$ ,  $20d$  and  $30d$ , respectively.

Generally, the prediction performance of our method is comparable to other adaptive approaches. In particular, it outperforms MSE and EIGF in approximating the Hartman ( $f_2$ ) and Gramacy & Lee ( $f_4$ ) functions. As can be seen, the sequential (black) and batch (orange) ES-LOO have similar performances such that in both algorithms the RMSE is monotonically (almost linearly) decreasing in all test problems. However, this is not the

case of other adaptive sampling approaches. The Hartmann function has four local minima and EIGF can stuck in one of them. The EIGF method has the best performance on the Friedman function ( $f_3$ ) and has the lowest accuracy in approximating other functions, especially  $f_4$ . The reason is that the main response change of  $f_4$  occurs near the right bound of the input space and EIGF puts more points there. The MICE algorithm shows a poor performance in predicting the test functions. However, it is the fastest algorithm as the criterion is based on a discrete representation. Other adaptive sampling methods could be implemented on similar discrete representation and they would then gain the speed up. It is observed that the points obtained by the MSE method fill the space almost uniformly in the Franke’s function and thus has a similar performance to the LHS method. However, MSE favours sampling more points on the boundary of the input space of the (6-dimensional)  $f_4$  function.

### 4.3 Real-world problems

We also tested our method on two real-world problems which are the 6-dimensional *output transformerless (OTL) circuit* and 7-dimensional *piston simulation* functions [4]. The former ( $f_{OTL}$ ) returns the midpoint voltage of a transformerless circuit and the latter ( $f_{piston}$ ) measures the cycle time that a piston takes to complete one cycle within a cylinder. The analytical expressions of  $f_{OTL}$  and  $f_{piston}$  and their design spaces are given in Appendix C. Figure 9 illustrates the results of comparing our proposed method with MSE, EIGF, MICE and LHS design in predicting the OTL circuit and piston simulation functions. The experimental setup is the same as explained in Section 4.1. The sequential (black) and batch (orange) ES-LOO have again similar performances and their RMSE criterion reduces steadily on both problems. As can be seen, ES-LOO is the best sampling approach for emulating the piston simulation function. The MSE approach does not work well in both problems, especially after almost  $10 \times d$  function evaluations. Based on our experiments, MSE is not recommended when the dimensionality of the problem is larger than five. While EIGF has the best performance on the OTL circuit problem, there is no improvement in the prediction accuracy of the emulator after  $10 \times d$  evaluations of the piston simulation function. MICE is the least successful algorithm in these two problems.

## 5 Conclusions

This paper deals with the problem of extending an initial design sequentially for training GP models. This is an important issue in the context of emulating computationally expensive computer codes where the goal is to approximate the underlying function with a minimum number of evaluations. An adaptive sampling scheme is presented based on the expected squared leave-one-out error (ES-LOO) which is used to identify “good” locations for future evaluations. Since the value of ES-LOO is only known at the design points, another GP model is applied to approximate it at unobserved sites. Then, the

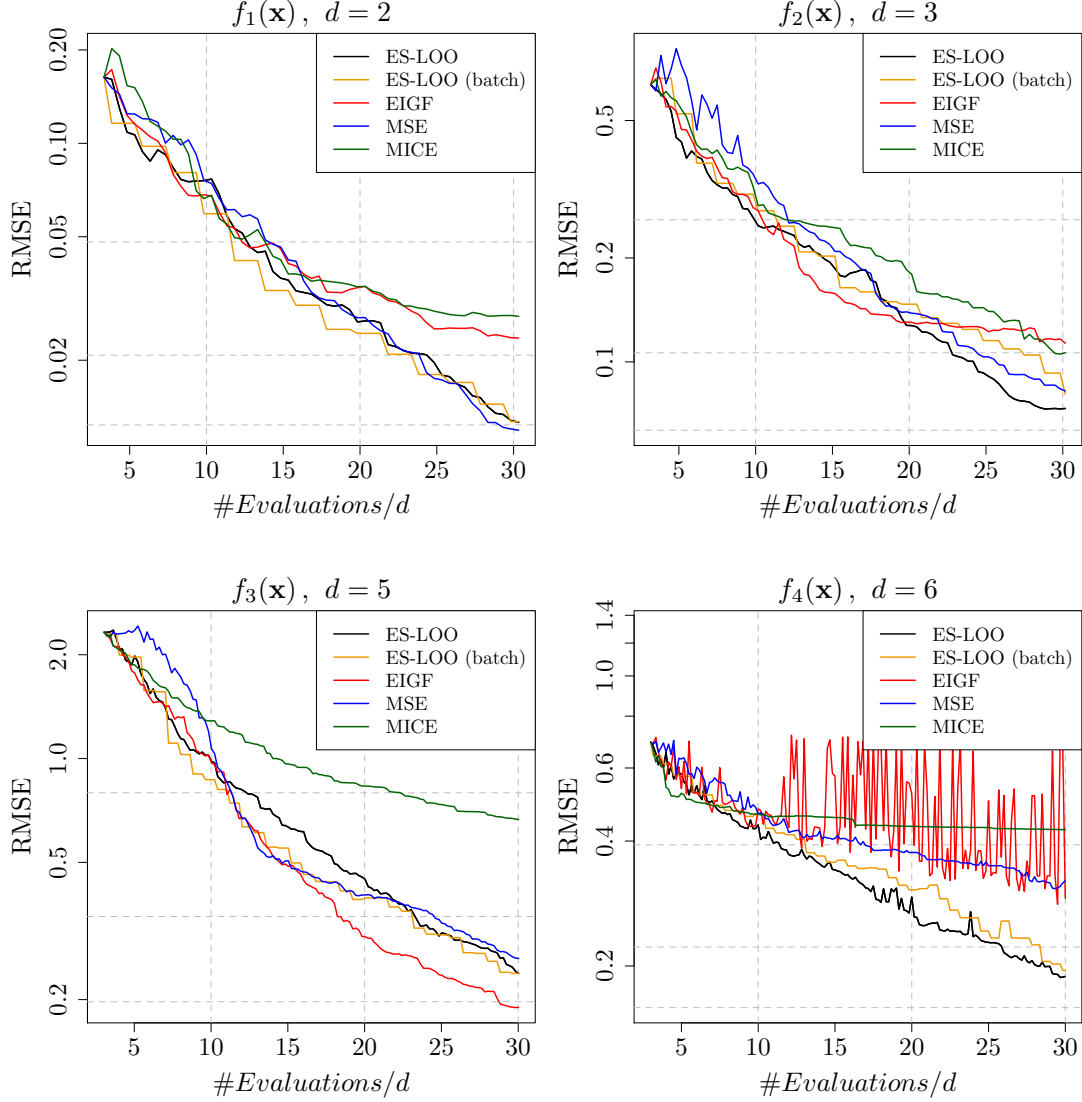


Figure 8: The median of ten RMSEs of our proposed approach ES-LOO: sequential (black) and batch with  $q = 4$  (orange), EIGF (red), MSE (blue) and MICE (green). Ten different initial DoEs of size  $3d$  are considered for each function; every method produces ten predictions based on them. The total budget is  $30d$ . The dashed grey lines show the median of RMSEs based on one-shot space-filling designs of sizes (from top to bottom):  $10d$ ,  $20d$  and  $30d$ , respectively. The  $y$ -axis is on logarithmic scale.

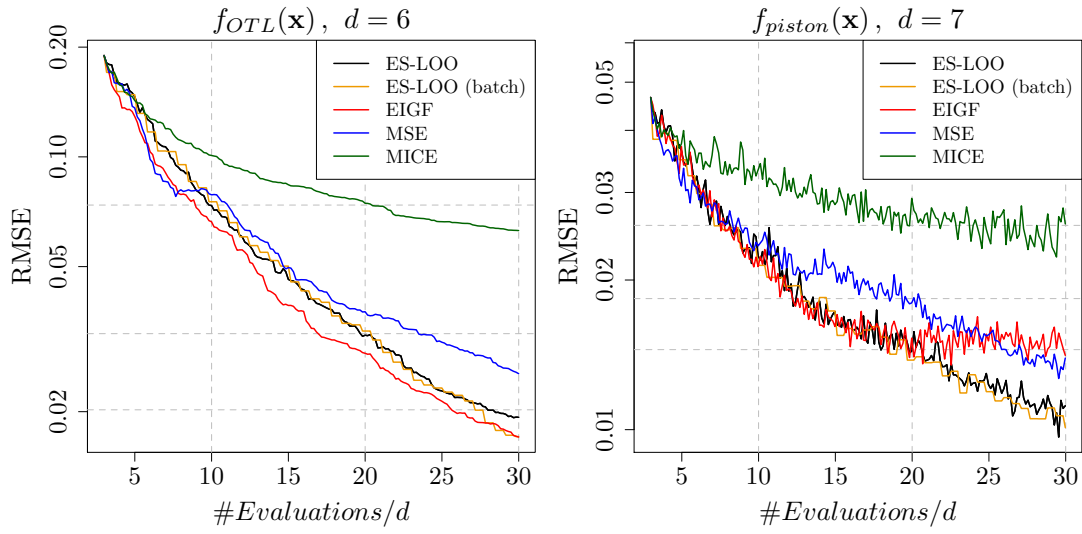


Figure 9: The median of ten RMSEs of our proposed approach ES-LOO: sequential (black) and batch with  $q = 4$  (orange), EIGF (red), MSE (blue) and MICE (green). The dashed grey lines show the median of RMSEs based on one-shot space-filling designs of sizes (from top to bottom):  $10d$ ,  $20d$  and  $30d$ , respectively. Size of initial design =  $3d$  and total budget =  $30d$ . The  $y$ -axis is on logarithmic scale.

pseudo expected improvement criterion is employed at each iteration to find the location of maximum of ES-LOO as the most promising point to improve the emulator. Pseudo expected improvement is obtained by multiplying the expected improvement criterion by a repulsion function. Once the new sample is chosen, it is added to the existing designs and the procedure is repeated until a stopping criterion is met. The proposed method can be easily promoted to a batch mode where at each iteration a set of input points is selected for evaluation. This can save the user time if parallel computing is available. Several test functions are used to test the capability of our method and the results are compared with other commonly used sampling techniques. The results show that our proposed adaptive sampling approach is promising.

## Acknowledgments

The authors gratefully acknowledge the financial support of the EPSRC via grant EP/N014391/1. The authors would like to thank the Isaac Newton Institute for Mathematical Sciences, Cambridge, for support and hospitality during the Uncertainty Quantification programme (UNQ) where work on this article was undertaken. We warmly thank Joakim Beck for discussions on the MICE algorithm.

## Appendix A MICE algorithm

In the MICE algorithm, the continuous design space is discretised into a finite grid  $\mathbf{X}_G \subseteq \mathcal{D}$  such that  $\mathbf{X}_G = \mathbf{X}_n \cup \mathbf{X}_{cand}$ . The latter is a set of candidate points on which the optimisation of the MI criterion is performed. The elements of  $\mathbf{X}_{cand}$  are regenerated at each iteration based on a maximin design scheme. The next sample location is obtained by the following optimisation problem

$$\mathbf{x}_{n+1} = \underset{\mathbf{x} \in \mathbf{X}_{cand}}{\operatorname{argmax}} s_n^2(\mathbf{x})/s_{G \setminus (n \cup \mathbf{x})}^2(\mathbf{x}; \tau^2), \quad (22)$$

wherein  $G \setminus (n \cup \mathbf{x})$  denotes  $\mathbf{X}_G \setminus (\mathbf{X}_n \cup \mathbf{x})$  and  $\tau^2$  is the nugget effect added to the correlation matrix of the GP fitted to  $\mathbf{X}_G \setminus (\mathbf{X}_n \cup \mathbf{x})$ . The inclusion of nugget prevents the denominator of Equation (22) approaching zero. The recommended value for the nugget parameter is one, although it can take any positive value in theory.

## Appendix B Test function expressions

The analytic expressions of four test functions used in our experiments are given below.

$$\begin{aligned} 1. \quad f_1(\mathbf{x}) = & 0.75 \exp\left(-\frac{(9x_1-2)^2}{4} - \frac{(9x_2-2)^2}{4}\right) + 0.75 \exp\left(-\frac{(9x_1+1)^2}{49} - \frac{9x_2+1}{10}\right) \\ & + 0.5 \exp\left(-\frac{(9x_1-7)^2}{4} - \frac{(9x_2-3)^2}{4}\right) - 0.2 \exp(-(9x_1-4)^2 - (9x_2-7)^2). \end{aligned}$$

2.  $f_2(\mathbf{x}) = -\sum_{i=1}^4 \boldsymbol{\alpha}_i \exp\left(\sum_{j=1}^3 \mathbf{A}_{ij} (x_j - \mathbf{P}_{ij})^2\right)$  where  $\boldsymbol{\alpha} = (1, 1.2, 3, 3.2)^\top$ ,

$$\mathbf{A} = \begin{bmatrix} 3 & 10 & 30 \\ 0.1 & 10 & 35 \\ 3 & 10 & 30 \\ 0.1 & 10 & 35 \end{bmatrix}, \quad \mathbf{P} = 10^{-4} \begin{bmatrix} 3689 & 1170 & 2673 \\ 4699 & 4387 & 7470 \\ 1091 & 8732 & 5547 \\ 381 & 5743 & 8828 \end{bmatrix}.$$

3.  $f_3(\mathbf{x}) = 10 \sin(\pi x_1 x_2) + 20(x_3 - 0.5)^2 + 10x_4 + 5x_5$ .

4.  $f_4(\mathbf{x}) = \exp(\sin([0.9(x_1 + 0.48))]^{10})) + x_2 x_3 + x_4$ .

## Appendix C Real-world function expressions

**OTL circuit function** The function  $f_{OTL}$  is defined as

$$f_{OTL}(\mathbf{x}) = \frac{(V_{b1} + 0.74)\beta(R_{c2} + 9)}{\beta(R_{c2} + 9) + R_f} + \frac{11.35R_f}{\beta(R_{c2} + 9) + R_f} + \frac{0.74R_f\beta(R_{c2} + 9)}{(\beta(R_{c2} + 9) + R_f)R_{c1}},$$

where  $V_{b1} = \frac{12R_{b2}}{R_{b1} + R_{b2}}$ . The input variables of  $f_{OTL}$  are:

- $R_{b1} \in [50, 150]$  is the resistance  $b_1$  (K-Ohms)
- $R_{b2} \in [25, 70]$  is the resistance  $b_2$  (K-Ohms)
- $R_f \in [0.5, 3]$  is the resistance  $f$  (K-Ohms)
- $R_{c1} \in [1.2, 2.5]$  is the resistance  $c_1$  (K-Ohms)
- $R_{c2} \in [0.25, 1.2]$  is the resistance  $c_2$  (K-Ohms)
- $\beta \in [50, 300]$  is the current gain  $c_1$  (Amperes).

**Piston simulation function** The function  $f_{piston}$  is defined as

$$f_{piston}(\mathbf{x}) = 2\pi \sqrt{\frac{M}{k + S^2 \frac{P_0 V_0 T_a}{T_0 V^2}}}, \quad \text{where } V = \frac{S}{2k} \left( \sqrt{A^2 + 4k \frac{P_0 V_0}{T_0} T_a} - A \right),$$

$$A = P_0 S + 19.62M - \frac{kV_0}{S}.$$

The input variables of  $f_{piston}$  are:

- $M \in [30, 60]$  is the piston weight (kg)
- $S \in [0.005, 0.020]$  is the piston surface area ( $m^2$ )

- $V_0 \in [0.002, 0.010]$  is the initial gas volume ( $m^3$ )
- $k \in [1000, 5000]$  is the spring coefficient (N/m)
- $P_0 \in [90000, 110000]$  is the atmospheric pressure ( $N/m^2$ )
- $T_a \in [290, 296]$  is the ambient temperature (K)
- $T_0 \in [340, 360]$  is the filling gas temperature (K).

## References

- [1] V. Aute, K. Saleh, O. Abdelaziz, S. Azarm, and R. Radermacher. Cross-validation based single response adaptive design of experiments for kriging metamodeling of deterministic computer simulations. *Structural and Multidisciplinary Optimization*, 48(3):581–605, 2013.
- [2] Gregory A. Banyay, Michael D. Shields, and John C. Brigham. Efficient global sensitivity analysis for flow-induced vibration of a nuclear reactor assembly using kriging surrogates. *Nuclear Engineering and Design*, 341:1 – 15, 2019.
- [3] J. Beck and S. Guillas. Sequential design with mutual information for computer experiments (MICE): Emulation of a tsunami model. *SIAM/ASA Journal on Uncertainty Quantification*, 4(1):739–766, 2016.
- [4] Einat Neumann Ben-Ari and David M. Steinberg. Modeling data from computer experiments: An empirical comparison of kriging with mars and projection pursuit regression. *Quality Engineering*, 19(4):327–338, 2007.
- [5] M. Ben Salem, O. Roustant, F. Gamboa, and L. Tomaso. Universal prediction distribution for surrogate models. *SIAM/ASA Journal on Uncertainty Quantification*, 5(1):1086–1109, 2017.
- [6] G. E. P. Box and J. S. Hunter. The  $2^{k-p}$  fractional factorial designs part ii. *Technometrics*, 3(4):449–458, 1961.
- [7] Eric Brochu, Vlad M. Cora, and Nando de Freitas. A tutorial on Bayesian optimization of expensive cost functions, with application to active user modeling and hierarchical reinforcement learning. *CoRR*, abs/1012.2599, 2010.
- [8] Olivier Dubrule. Cross validation of kriging in a unique neighborhood. *Journal of the International Association for Mathematical Geology*, 15(6):687–699, 1983.
- [9] Delphine Dupuy, Céline Helbert, and Jessica Franco. DiceDesign and DiceEval: two R packages for design and analysis of computer experiments. *Journal of Statistical Software*, 65(11):1–38, 2015.

- [10] Jerome H. Friedman. Multivariate adaptive regression splines. *The Annals of Statistics*, 19(1):1–67, 1991.
- [11] Sushant S. Garud, Iftekhar A. Karimi, and Markus Kraft. Design of computer experiments: A review. *Computers & Chemical Engineering*, 106:71 – 95, 2017. ESCAPE-26.
- [12] Andrew Gelman, John Carlin, Hal Stern, David Dunson, Aki Vehtari, and Donald Rubin. Bayesian Data Analysis, Third Edition (Chapman & Hall/CRC Texts in Statistical Science), 2013.
- [13] Robert B. Gramacy and Herbert K. H. Lee. Adaptive design and analysis of supercomputer experiments. *Technometrics*, 51(2):130–145, 2009.
- [14] Ben Haaland and Peter Z. G. Qian. Accurate emulators for large-scale computer experiments. *The Annals of Statistics*, 39(6):2974–3002, 2011.
- [15] Momin Jamil and Xin-She Yang. A literature survey of benchmark functions for global optimization problems. *International Journal of Mathematical Modelling and Numerical Optimisation*, 4(2):150–194, 2013.
- [16] Ruichen Jin, Wei Chen, and Agus Sudjianto. On sequential sampling for global meta-modeling in engineering design. In *Design Engineering Technical Conferences And Computers and Information in Engineering*, volume 2, pages 539–548, 2002.
- [17] M.E. Johnson, L.M. Moore, and D. Ylvisaker. Minimax and maximin distance designs. *Journal of Statistical Planning and Inference*, 26(2):131 – 148, 1990.
- [18] Donald R. Jones. A taxonomy of global optimization methods based on response surfaces. *Journal of Global Optimization*, 21(4):345–383, Dec 2001.
- [19] Donald R. Jones, Matthias Schonlau, and William J. Welch. Efficient global optimization of expensive black-box functions. *Journal of Global Optimization*, 13(4):455–492, 1998.
- [20] V. Roshan Joseph. Space-filling designs for computer experiments: A review. *Quality Engineering*, 28(1):28–35, 2016.
- [21] Crombecq Karel, Dirk Gorissen, Dirk Deschrijver, and Tom Dhaene. A novel hybrid sequential design strategy for global surrogate modeling of computer experiments. *SIAM Journal on Scientific Computing*, 33(4):1948–1974, 2011.
- [22] J.R. Koehler and A.B. Owen. Computer experiments. In *Design and Analysis of Experiments*, volume 13 of *Handbook of Statistics*, pages 261 – 308. Elsevier, 1996.

- [23] Andreas Krause, Ajit Singh, and Carlos Guestrin. Near-optimal sensor placements in Gaussian processes: Theory, efficient algorithms and empirical studies. *Journal of Machine Learning Research*, 9:235–284, February 2008.
- [24] Chen Quin Lam. *Sequential adaptive designs in computer experiments for response surface model fit*. PhD thesis, Columbus, OH, USA, 2008. AAI3321369.
- [25] Loic Le Gratiet and Claire Cannamela. Kriging-based sequential design strategies using fast cross-validation techniques with extensions to multi-fidelity computer codes. *arXiv e-prints*, page arXiv:1210.6187, 2012.
- [26] Genzi Li, Vikrant Aute, and Shapour Azarm. An accumulative error based adaptive design of experiments for offline metamodeling. *Structural and Multidisciplinary Optimization*, 40(1):137–157, 2009.
- [27] D. Liu, A. Litvinenko, C. Schillings, and V. Schulz. Quantification of airfoil geometry-induced aerodynamic uncertainties—comparison of approaches. *SIAM/ASA Journal on Uncertainty Quantification*, 5(1):334–352, 2017.
- [28] Haitao Liu, Yew-Soon Ong, and Jianfei Cai. A survey of adaptive sampling for global metamodeling in support of simulation-based complex engineering design. *Structural and Multidisciplinary Optimization*, 57(1):393–416, 2018.
- [29] Haitao Liu, Shengli Xu, Ying Ma, Xudong Chen, and Xiaofang Wang. An adaptive Bayesian sequential sampling approach for global metamodeling. *Journal of Mechanical Design*, 138(1), 2015.
- [30] Jay Martin and Timothy Simpson. Use of adaptive metamodeling for design optimization. In *9th AIAA/ISSMO Symposium on Multidisciplinary Analysis and Optimization*, pages 1–9, 2002.
- [31] M. D. McKay, R. J. Beckman, and W. J. Conover. A comparison of three methods for selecting values of input variables in the analysis of output from a computer code. *Technometrics*, 21(2):239–245, 1979.
- [32] Hossein Mohammadi. *Kriging-based black-box global optimization: analysis and new algorithms*. PhD thesis, École Nationale Supérieure des Mines de Saint-Étienne, France, 2016.
- [33] Radford M. Neal. Regression and classification using Gaussian process priors. pages 475–501. Bayesian Statistics 6, Oxford University Press, 1998.
- [34] Art B. Owen. Orthogonal arrays for computer experiments, integration and visualization. *Statistica Sinica*, 2(2):439–452, 1992.

- [35] V. Picheny, D. Ginsbourger, O. Roustant, R. T. Haftka, and N. H. Kim. Adaptive designs of experiments for accurate approximation of a target region. *Journal of Mechanical Design*, 132(7):1–9, 2010.
- [36] W. Ponweiser, T. Wagner, and M. Vincze. Clustered multiple generalized expected improvement: A novel infill sampling criterion for surrogate models. In *2008 IEEE Congress on Evolutionary Computation (IEEE World Congress on Computational Intelligence)*, pages 3515–3522, 2008.
- [37] Luc Pronzato and Werner G. Müller. Design of computer experiments: space filling and beyond. *Statistics and Computing*, 22(3):681–701, 2012.
- [38] Carl Edward Rasmussen and Christopher K. I. Williams. *Gaussian processes for machine learning (adaptive computation and machine learning)*. The MIT Press, 2005.
- [39] Olivier Roustant, David Ginsbourger, and Yves Deville. DiceKriging, DiceOptim: Two R packages for the analysis of computer experiments by kriging-based metamodeling and optimization. *Journal of Statistical Software*, 51(1):1–55, 2012.
- [40] Jerome Sacks, William J. Welch, Toby J. Mitchell, and Henry P. Wynn. Design and analysis of computer experiments. *Statistical Science*, 4(4):409–423, 1989.
- [41] T. J. Santner, Williams B., and Notz W. *The design and analysis of computer experiments*. Springer-Verlag, 2003.
- [42] Matthias Schonlau. *Computer experiments and global optimization*. PhD thesis, University of Waterloo, 1997.
- [43] Razi Sheikholeslami and Saman Razavi. Progressive latin hypercube sampling: an efficient approach for robust sampling-based analysis of environmental models. *Environmental Modelling & Software*, 93:109 – 126, 2017.
- [44] M. C. Shewry and H. P. Wynn. Maximum entropy sampling. *Journal of Applied Statistics*, 14(2):165–170, 1987.
- [45] T.W. Simpson, J.D. Poplinski, P. N. Koch, and J.K. Allen. Metamodels for computer-based engineering design: Survey and recommendations. *Engineering with Computers*, 17(2):129–150, 2001.
- [46] Ian Vernon, Junli Liu, Michael Goldstein, James Rowe, Jen Topping, and Keith Lindsey. Bayesian uncertainty analysis for complex systems biology models: emulation, global parameter searches and evaluation of gene functions. *BMC Systems Biology*, 12(1):1, 2018.

- [47] Victoria Volodina and Daniel Williamson. Diagnostics-driven nonstationary emulators using kernel mixtures. *SIAM/ASA Journal on Uncertainty Quantification*, 8(1):1–26, 2020.
- [48] Daniel Williamson. Exploratory ensemble designs for environmental models using k-extended Latin Hypercubes. *Environmetrics*, 26(4):268–283, 2015.
- [49] Dawei Zhan, Jiachang Qian, and Yuansheng Cheng. Pseudo expected improvement criterion for parallel EGO algorithm. *Journal of Global Optimization*, 68(3):641–662, 2017.